CrossMark

J. Fluid Mech. (2020), *vol*. 903, R4, doi:10.1017/jfm.2020.718



Exact relations between Rayleigh–Bénard and rotating plane Couette flow in two dimensions

Bruno Eckhardt[1], **Charles R. Doering**[2] **and Jared P. Whitehead**[3],†

[1]Fachbereich Physik, Philipps-Universität Marburg, D-35032 Marburg, Germany

[2]Center for the Study of Complex Systems, Department of Mathematics and Department of Physics, University of Michigan, Ann Arbor, MI 48109, USA

[3]Department of Mathematics, Brigham Young University, Provo, UT 84602, USA

(Received 16 June 2020; revised 22 July 2020; accepted 10 August 2020)

Rayleigh–Bénard convection (RBC) and Taylor–Couette flow (TCF) are two paradigmatic fluid dynamical systems frequently discussed together because of their many similarities despite their different geometries and forcing. Often these analogies require approximations, but in the limit of large radii where TCF becomes rotating plane Couette flow (RPC) exact relations can be established. When the flows are restricted to two spatial independent variables, there is an exact specification that maps the three velocity components in RPC to the two velocity components and one temperature field in RBC. Using this, we deduce several relations between both flows: (i) heat and angular momentum transport differ by $(1 - R_\Omega)$, explaining why angular momentum transport is not symmetric around $R_\Omega = 1/2$ even though the relation between Ra, the Rayleigh number, and R_Ω, a non-dimensional measure of the rotation, has this symmetry. This relationship leads to a predicted value of R_Ω that maximizes the angular momentum transport that agrees remarkably well with existing numerical simulations of the full three-dimensional system. (ii) One variable in both flows satisfies a maximum principle, i.e. the fields' extrema occur at the walls. Accordingly, backflow events in shear flow cannot occur in this quasi two-dimensional setting. (iii) For free-slip boundary conditions on the axial and radial velocity components, previous rigorous analysis for RBC implies that the azimuthal momentum transport in RPC is bounded from above by $Re_S^{5/6}$, where Re_S is the shear Reynolds number, with a scaling exponent smaller than the anticipated Re_S^1.

Key words: Bénard convection, Taylor–Couette flow

† Email address for correspondence: whitehead@mathematics.byu.edu

© The Author(s), 2020. Published by Cambridge University Press

https://doi.org/10.1017/jfm.2020.718 Published online by Cambridge University Press

1. Introduction

Rayleigh–Bénard convection (RBC), the buoyancy-driven motion of a fluid heated from below, and Taylor–Couette flow (TCF) wherein a fluid is sheared between two rigid differentially rotating cylinders, are paradigms in the physical and engineering sciences and have been studied extensively to gain insights into turbulence. It has long been recognized that despite their qualitative differences they share many features, both physically and mathematically. Indeed, the comparison between RBC and TCF goes back nearly to the original definition of these canonical fluids problems. As stated in Jeffreys (1928):

> *Prof. G. I. Taylor and Major A. R. Low have both suggested to me that there should be an analogy between the conditions in a layer of liquid heated below and in a liquid between two coaxial cylinders rotating at different rates.*

Jeffreys (1928) considered this analogy in the context of linear stability of the basic states (pure conduction for RBC and axisymmetric laminar flow for TCF), a line of reasoning quantified further by Chandrasekhar (1961). Subsequent investigations into the onset of convective and shear turbulence have led to significant advances in pattern formation, the mathematical theory of chaotic and nonlinear dynamics, and insight into the influence and interaction of linear and nonlinear instabilities (Gollub & Swinney 1975; Ahlers & Behringer 1978; Manneville 2010; Chossat & Iooss 2012).

This analogy was first extended to turbulent flow by Bradshaw (1969), with further contributions due to Dubrulle & Hersant (2002) and Eckhardt, Grossmann & Lohse (2007*a*,*b*). The basis for these analogies is the identification and comparison of corresponding quantities between the two systems, such as the total dissipation and global transport of physically motivated quantities, such as heat or angular momentum. The similarities between RBC and TCF then lead to relations between the non-dimensional parameters of the system and allow for direct comparisons of the pertinent physical quantities. As noted by Brauckmann, Eckhardt & Schumacher (2017) and demonstrated in direct numerical simulations, the similarity between TCF and RBC gives rise to similar behaviour not only in the mean properties but also in the fluctuations, indicating that an even more precise comparison may be possible.

There are profound differences between these two canonical problems as well. In particular, RBC has a parameter with no correspondence in the TCF or rotating plane Couette flow (RPC, i.e. the limit of vanishing curvature in TCF) setting, namely the Prandtl number. The dynamics and analysis of RBC in the large Prandtl number limit – see, e.g. Doering, Otto & Reznikoff (2006), Otto & Seis (2011) and Whitehead & Doering (2012) – has no counterpart in TCF or RPC. Physically relevant boundary conditions are also uniquely identified between convection and shear-driven flows. For the specific case of two-dimensional (2-D) RBC between free-slip isothermal boundaries, for example, Whitehead & Doering (2011) showed that the convective heat flux at arbitrary Prandtl number is bounded above by the Rayleigh number to the $5/12$ power, ruling out the conjectured 'ultimate' $\sim Ra^{1/2}$ scaling in this setting. We can identify a corresponding situation in RPC under some additional assumptions, where the azimuthal momentum transport is bounded above by the Reynolds number to the (perhaps unexpected) $5/6$ power.

Correspondence between RBC and RPC also extends into the realm of rigorous mathematical analysis due to the vanishing of all geometric curvature terms in the limit of TCF approaching RPC (see Dubrulle *et al.* (2005) for a detailed examination of this limit). Energy stability of the conductive state in RBC corresponds precisely

https://doi.org/10.1017/jfm.2020.718 Published online by Cambridge University Press

(up to the appropriate change of variables) to energy stability of the laminar plane-parallel solutions of RPC. As an extension of energy stability, the original upper bound analysis for statistically stationary heat transport in RBC introduced by Howard (1963) transfers directly via relabelling and rescaling of variables to an upper bound analysis for the energy dissipation rate in RPC (Busse 1969; Howard 1972). The subsequently developed background method for producing upper bounds (Doering & Constantin 1992) shares the same exact correspondence (Doering & Constantin 1994, 1996; Plasting & Kerswell 2003). Both Howard's approach and the background method are easily adapted to the cylindrical setting of TCF (Nickerson 1969; Constantin 1994).

The relation between RBC and TCF is complicated by the fact that the rotation in TCF does not have a corresponding analogy in RBC. The comparison between the two flows shown in Brauckmann *et al.* (2017) was, therefore, based on correspondences in mean transport. Here, we discuss consequences of an exact relation between 2-D RBC and azimuthally symmetric TCF in the limit of a large cylindrical radius where it becomes rotating plane Couette flow (RPC) (Nagata 1986; Faisst & Eckhardt 2000; Nagata 2013). We emphasize at this point that for the geometry and restrictions described below, the resulting relations are exact, and without approximation. That is to say, the 2-D RBC system has an exact analogue in 2D3C (2-dimensional, 3-component) RPC, the 2-D TCF system in the limit of large radii relative to the gap size.

2. Derivation of the relations

Exact relations between TCF and RBC are only possible if the spatial variables are restricted to two dimensions, as otherwise the number of dependent variables does not match. In the full three-dimensional (3-D) setting, RBC has three velocity components and one temperature, while TCF has only three components of velocity (both systems also have a pressure gradient). Fully 2-D RBC has two components of velocity and a temperature, while TCF or RPC that is independent of the azimuthal spatial coordinate will have three components of velocity, with the azimuthal velocity playing the role of the temperature in RBC. Some historical context for the analogy between RBC and TCF as well as comments on how it fails in three dimensions are explained in Veronis (1970). The comparison between the two systems is relatively straightforward (the precise formulation of the analogy is given in an appendix to Nagata 2013), but for completeness we repeat the relevant derivation, the main task in the following being to keep track of the transformations in the dependent and independent variables.

2.1. *2-D Rayleigh–Bénard*

For the 2-D Rayleigh–Bénard system, there are two velocity fields and a temperature field. We take x_1 as the spanwise (horizontal) direction and impose periodicity in this direction, x_2 is an additional horizontal direction that is absent in the 2-D case, and x_3 points in the direction of gravity The velocity field then has components $\boldsymbol{u} = (u(x_1, x_3), w(x_1, x_3))$ that are restricted to be incompressible, $\partial_1 u + \partial_3 w = 0$. The boundary conditions on the velocity field are usually rigid $u = w = 0$, or free-slip ($w = 0$ and $\partial_3 u = 0$) at the top and bottom plates. The derivations in this section do not depend on the specific boundary conditions on $\boldsymbol{u}$; however, in § 3.3, we will consider free-slip boundary conditions specifically and the implications on maximal heat transport (figure 1).

The dimensional temperature is $T = T(x_1, x_3)$ and it satisfies the boundary conditions $T(x_3 = 0) = T_0 + \delta T$ and $T(x_3 = d) = T_0$, i.e. the temperature at the bottom plate is higher by the fixed amount δT. Using the Boussinesq approximation,

https://doi.org/10.1017/jfm.2020.718 Published online by Cambridge University Press

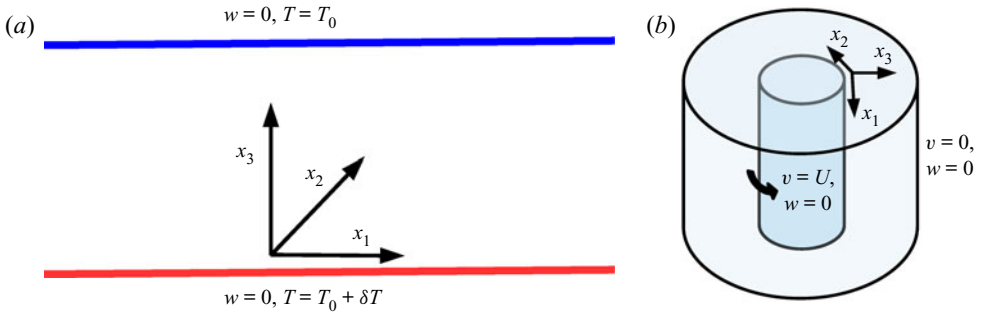


FIGURE 1. (*a*) The geometry, choice of coordinates, and generic boundary conditions for the Rayleigh–Bénard set-up (particular boundary conditions on u depend on the physical setting, i.e. stress-free versus no-slip). (*b*) The same for Taylor–Couette.

the equations of motion are

$$\partial_t u + (\boldsymbol{u}\cdot\boldsymbol{\nabla})u + 1/\rho\partial_1 p = \nu\Delta u, \tag{2.1a}$$

$$\partial_t w + (\boldsymbol{u}\cdot\boldsymbol{\nabla})w + 1/\rho\partial_3 p = \nu\Delta w + g\beta T, \tag{2.1b}$$

$$\partial_t T + (\boldsymbol{u}\cdot\boldsymbol{\nabla})T = \kappa\Delta T, \tag{2.1c}$$

combined with incompressibility: $\boldsymbol{\nabla}\cdot\boldsymbol{u} = 0$, where $\boldsymbol{\nabla} = (\partial_1, \partial_3)$, and $\Delta = \partial_{11}^2 + \partial_{33}^2$. The other variables are the kinematic viscosity ν, the thermal diffusivity κ, the density ρ, the expansion coefficient β and the gravitational constant g. As mentioned above, $x_3 = 0$ is the bottom plate and $x_3 = d$ the top plate. In the absence of convection, the temperature displays a linear profile, $T_0(x_3) = \delta T\,(1 - (x_3/d))$. This non-convective buoyancy is balanced by the pressure field $p_0(x_3) = \beta g\delta T x_3(1 - (x_3/(2d)))$. We decompose the full temperature field according to $T(x_1, x_3, t) = T_0(x_3) + \theta(x_1, x_3, t)$. Decomposing the pressure in a similar manner, but using p to now refer to perturbations about the laminar pressure p_0, we can derive the equations for the deviation θ from the diffusive profile:

$$\partial_t u + (\boldsymbol{u}\cdot\boldsymbol{\nabla})u + \partial_1 p = \nu\Delta u, \tag{2.2a}$$

$$\partial_t w + (\boldsymbol{u}\cdot\boldsymbol{\nabla})w + \partial_3 p = \nu\Delta w + g\beta\theta, \tag{2.2b}$$

$$\partial_t\theta + (\boldsymbol{u}\cdot\boldsymbol{\nabla})\theta - \delta T(w/d) = \kappa\Delta\theta, \tag{2.2c}$$

coupled with incompressibility for the velocity field.

In RBC, dimensionless variables for temperature, length and time are based on the temperature difference δT, the height d and the thermal diffusivity κ. Then in the non-dimensional setting, we have the system:

$$\partial_t u + (\boldsymbol{u}\cdot\boldsymbol{\nabla})u + \partial_1 p = Pr\Delta u, \tag{2.3a}$$

$$\partial_t w + (\boldsymbol{u}\cdot\boldsymbol{\nabla})w + \partial_3 p = Pr\Delta w + PrRa\theta, \tag{2.3b}$$

$$\partial_t\theta + (\boldsymbol{u}\cdot\boldsymbol{\nabla})\theta = w + \Delta\theta, \tag{2.3c}$$

again coupled with incompressibility of $\boldsymbol{u}$, and where the Rayleigh number is given by $Ra = (g\beta\delta T\, d^3)/(\kappa\nu)$, and the Prandtl number $Pr = \nu/\kappa$. We now wish to re-scale the 2-D RPC system so that it has the same functional form as these three equations. As we see, the analogy is exact only when $Pr = 1$, and if we carefully re-scale the azimuthal component of the velocity field so that it appears in the same way as the temperature fluctuations.

https://doi.org/10.1017/jfm.2020.718 Published online by Cambridge University Press

2.2. 2D3C plane Couette flow

The full Taylor–Couette system consists of three velocity components that are linked by incompressibility. In order to split off a temperature-like component, we consider a restricted geometry where the fields do not depend on the azimuthal spatial coordinate, and we investigate the limit of large radius relative to the gap size, i.e. the limit of zero curvature. In this set-up, the azimuthal velocity component decouples and can be re-scaled to resemble the temperature fluctuations from RBC.

The radial direction in the TCF system is analogous to the gravitational direction in the RBC system, so that the x_3 direction becomes the radial one. The neutral direction for the flow is the axial one, which, therefore, is referred to as the x_1 direction, and in which we assume the flow to be periodic. Finally, the azimuthal component becomes the x_2 direction. Invariance of the azimuthal position then implies that the velocity field has dependencies $(u(x_1, x_3), v(x_1, x_3), w(x_1, x_3))$. In a frame of reference rotating with frequency Ω around the x_1-axis, the system then becomes

$$\partial_t u + (\boldsymbol{u} \cdot \boldsymbol{\nabla})u + \partial_1 p = \nu \Delta u, \tag{2.4a}$$

$$\partial_t w + (\boldsymbol{u} \cdot \boldsymbol{\nabla})w + \partial_3 p = \nu \Delta w + 2\Omega v, \tag{2.4b}$$

$$\partial_t v + (\boldsymbol{u} \cdot \boldsymbol{\nabla})v = -2\Omega w + \nu \Delta v, \tag{2.4c}$$

together with incompressibility, $\partial_1 u + \partial_3 w = 0$.

The domain is bounded by two walls, i.e. the inner and outer cylinders, which we denote as $x_3 = 0$ and $x_3 = d$, that are parallel to the $x_1 - x_2$ plane. Between the plates, there is a mean shear, maintained by moving the walls at constant speed U in the x_2-direction. This yields the boundary conditions $v(x_3 = 0) = U$ and $v(x_3 = d) = 0$, which gives rise to a linear laminar velocity profile, $v(x_3) = U(1 - (x_3/d))$. The typical physically motivated boundary condition on the other components of velocity is the no-slip condition, meaning that the other components of the velocity field vanish identically at these walls. In § 3.3, we discuss the effect of considering a slippery boundary for v and w, a condition that is not as physically relevant but is more conducive to analysis.

As in the case of RBC, we are primarily concerned with deviations v' from the linear profile, that is

$$v(x_1, x_3, t) = U(1 - (x_3/d)) + v'(x_1, x_3, t), \tag{2.5}$$

where v' is the dimensional form of the deviations. The linear part in v is absorbed in the pressure (compensating the centrifugal forces) as was done for RBC, so that only the fluctuations remain. The equation for the azimuthal component then becomes

$$\partial_t v' + (\boldsymbol{u} \cdot \boldsymbol{\nabla})v' - (U/d)w = -2\Omega w + \nu \Delta v'. \tag{2.6}$$

The contribution from the normal velocity has a prefactor proportional to $(U - 2\Omega d)$ that can be absorbed in the azimuthal component v' with the rescaling

$$v' = (U - 2\Omega d)\theta. \tag{2.7}$$

Note that this scaling introduces a partial asymmetry between the velocity components since it affects only one and not all three components. It is, therefore, not reasonable for the full 3-D system.

The identification of this renormalization of the azimuthal velocity fluctuations to the variable θ is intentional, as this normalized dependent variable is identified with the

https://doi.org/10.1017/jfm.2020.718 Published online by Cambridge University Press

	Rayleigh–Bénard	Plane Couette
Corresponding velocities	u, w	u, w
Temperature and azimuthal velocity	θ	$(U/d - 2\Omega)v$
Prandtl number	Pr	1
Rayleigh, Reynolds, and rotation numbers	Ra	$Re_S^2 R_\Omega (1 - R_\Omega)$
Nusselt numbers	$Nu_T - 1$	$(Nu_S - 1)/(1 - R_\Omega)$

TABLE 1. Exact relations between the azimuthally independent RPC system and 2-D RBC.

temperature fluctuations for the 2-D RBC system described above. With this definition of θ, the dimensional equation for the azimuthal velocity becomes

$$\partial_t \theta + (\boldsymbol{u} \cdot \boldsymbol{\nabla})\theta = d/w + \nu \Delta \theta \tag{2.8}$$

and the evolution of u and w in RPC become

$$\partial_t u + (\boldsymbol{u} \cdot \boldsymbol{\nabla})u + \partial_1 p = \nu \Delta u, \tag{2.9a}$$

$$\partial_t w + (\boldsymbol{u} \cdot \boldsymbol{\nabla})w + \partial_3 p = \nu \Delta w + 2\Omega((U/d) - 2\Omega)\theta \tag{2.9b}$$

Now we introduce dimensionless variables for the rest of the system using the gap d and the viscosity ν to generate spatial and temporal scales (and, hence, velocity as well), which give the shear Reynolds number $Re_S = Ud/\nu$, and the rotation number, $R_\Omega = 2\Omega d/U$. Then the full non-dimensional equations for RPC become

$$\partial_t u + (\boldsymbol{u} \cdot \boldsymbol{\nabla})u + \partial_1 p = \Delta u, \tag{2.10a}$$

$$\partial_t w + (\boldsymbol{u} \cdot \boldsymbol{\nabla})w + \partial_3 p = \Delta w + Re_S^2 R_\Omega (1 - R_\Omega)\theta, \tag{2.10b}$$

$$\partial_t \theta + (\boldsymbol{u} \cdot \boldsymbol{\nabla})\theta = w + \Delta \theta, \tag{2.10c}$$

which is formally identical to the RBC case identifying $Pr = 1$ and the Taylor number Ta with the Rayleigh number, $Ra = Re_S^2 R_\Omega (1 - R_\Omega)$. This derivation did not use the boundary conditions on the velocity field so that it is valid for both rigid and free-slip boundary conditions or any mixture thereof.

The exact relationships between the RPC and RBC systems considered here are summarized in table 1.

3. Consequences of the relation between RPC and RBC

3.1. *Heat and momentum transport*

The first set of consequences we discuss here stem from the heat and angular momentum transport, and will be valid for all boundary conditions on the velocity fields u and w. In RBC, the temperature difference drives convection, which enhances the heat transport between the plates. The Nusselt number measures the heat transport in units of the diffusive heat transport, and is computed as $Nu_T = 1 + \overline{w\theta}$, where $\overline{\cdot}$ refers to an average in time, and across the x_1 direction.

For RPC, the azimuthal momentum transport is derived by averaging the dimensional equation for the azimuthal velocity in the x_1 direction and in time: $\partial_3 \overline{wv} = 2\Omega \bar{w} + \nu \partial_{33}^2 \bar{v}$.

https://doi.org/10.1017/jfm.2020.718 Published online by Cambridge University Press

Integrating this once in x_3 then gives the momentum current

$$J = \overline{wv} - \nu\partial_3\bar{v} = -\nu\partial_3\ \bar{v}|_{x_3=0}\,, \tag{3.1}$$

which is independent of the position x_3 between the plates. Using the laminar profile and (2.7) for the azimuthal velocity and dividing J by the linear viscous drag $\nu U/d$, one arrives at the equivalent of the Nusselt number in RPC for the non-dimensional variables

$$Nu_S = 1 + \left(1 - \frac{2\Omega d}{U}\right)\overline{w\theta} = 1 + (1 - R_\Omega)\,\overline{w\theta}, \tag{3.2}$$

$$\Rightarrow Nu_S(Re_S, R_\Omega) - 1 = (1 - R_\Omega)(Nu_T(Ra) - 1). \tag{3.3}$$

Thus, while the relation between the parameters Ra in RBC and Ta in RPC is symmetric under the exchange R_Ω to $1 - R_\Omega$, the relation between heat and momentum transport is not. Remarkably, this connection predicts that Nu_S approaches the laminar value $Nu_S = 1$ for R_Ω approaching 1, for any value of Re_S.

The transport of momentum as a function of rotation number has been studied for different parameter values in both TCF and RPC. Assuming that the Nusselt number in RBC follows a scaling law $Nu_T \sim cRa^\alpha$ with an as yet undetermined exponent α and some constant c, we can obtain a scaling for Nu_S in terms of both Re_S and R_Ω and determine the maximal R_Ω. First, we observe that

$$\begin{aligned} Nu_S - 1 &\sim cRe_S^{2\alpha}R_\Omega^\alpha(1 - R_\Omega)^{1+\alpha} - 1 + R_\Omega \\ \Rightarrow \quad Nu_S &\sim R_\Omega + cRe_S^{2\alpha}R_\Omega^\alpha(1 - R_\Omega)^{1+\alpha}. \end{aligned} \tag{3.4}$$

For large Re_S, the first part can be neglected and the relation reduces to

$$Nu_S \sim c'R_\Omega^\alpha(1 - R_\Omega)^{1+\alpha}, \tag{3.5}$$

away from $R_\Omega = 0$ or $R_\Omega = 1$. Maximizing this transport over the rotation rate R_Ω (for $Re_S \gg 1$) leads to

$$R_{\Omega,m} \sim \frac{\alpha}{1 + 2\alpha}. \tag{3.6}$$

In one conjectured asymptotic regime of thermal convection (Spiegel 1963), it is expected that $\alpha = 1/2$ so that the maximal momentum transport would occur for $R_{\Omega,m} \sim 1/4$. The Reynolds numbers in numerical simulations and even in experiments are not high enough to reach this regime, and one resorts to Reynolds number dependent local scaling exponents. For RPC and $Re_S = 2 \times 10^4$, Salewski & Eckhardt (2015) find a maximum near $R_{\Omega,m} \approx 0.2$. The transition from TCF to RPC is discussed in Brauckmann *et al.* (2016), where it is shown that the maximum again appears near $R_{\Omega,m} \approx 0.2$ when the ratio of the radius of the inner cylinder to that of the outer cylinder is $\eta = 0.99$. This amounts to a ratio of angular velocities of $\mu = 0.9043$, which is remarkably close to $\mu = 0.9801$, which is the Rayleigh criterion for $R_\Omega = 1$ for this value of η. This observation is further cemented by the recent numerical and experimental results reported in Ezeta *et al.* (2020). Both sets of data (for TCF and RPC) are shown in figure 2 (blue symbols). This agreement with observations is remarkable because the derivation here is valid only for the 2-D setting with a rescaling of v that violates the natural scaling of the velocity fields, whereas the reported maxima of $R_\Omega \sim 0.2$ comes from numerical studies of the full 3-D flow. However, since rotation reduces the transverse components and enhances the azimuthally invariant parts, Brauckmann *et al.* (2016) also isolated the contribution of

https://doi.org/10.1017/jfm.2020.718 Published online by Cambridge University Press

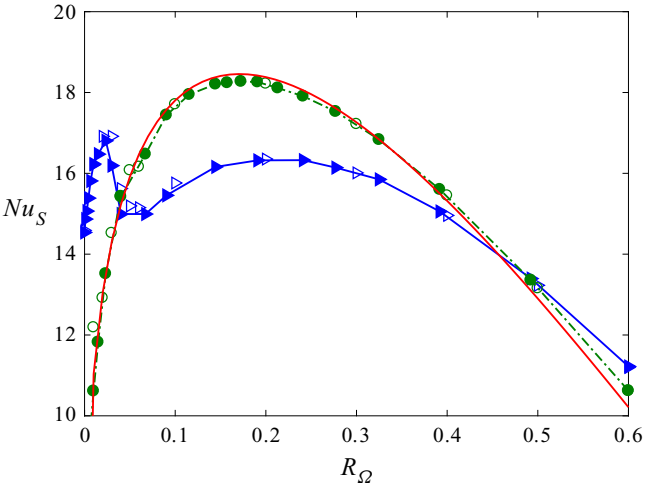


FIGURE 2. Nusselt number Nu_S for TCF and RPC versus rotation number R_Ω for $Re_S = 2 \times 10^4$, redrawn from figure 8(f) of Brauckmann, Salewski & Eckhardt (2016). The full symbols are for TCF at radius ratio $\eta = 0.99$, the open symbols are for RPC. The blue data are for the full 3-D flow; they have a broad maximum at $R_\Omega \approx 0.22$, and a narrow one for smaller R_Ω of a different origin (see Salewski & Eckhardt 2015; Brauckmann *et al.* 2016). The green data are obtained from the azimuthally invariant 2-D part of the flow. The continuous red line is a fit of the 2-D part to expression (3.5), with optimal parameters $\alpha = 0.26$ and $c = 37$ and a maximum near $R_\Omega \approx 0.18$, very close to the maximum obtained from (3.6).

the azimuthally invariant 2-D component of the flow, shown in figure 2 as the green data points. They show a maximum near $R_\Omega \approx 0.18$. Moreover, a fit of the 2-D contributions to the functional form (3.5) with $\alpha = 0.26$ approximates these data very well over essentially the entire range $0 < R_\Omega < 0.6$ for which data are available. This confirms that the 2-D analysis presented here adequately explains features of the 3-D flow, in this case, the momentum transport of the azimuthally invariant part of the flow. We note that $\alpha = 0.26$ is significantly less than either of the prevailing theoretical predictions for turbulent convection ($\alpha = 1/2$ and $\alpha = 1/3$). This may be due to the restriction to azimuthally invariant parts of the flow (2-D flow, see Whitehead & Doering (2011), for example), or it may be because $Re_S = 2 \times 10^4$ is not in the asymptotic regime where one of these expected laws takes hold. In either case, the general form of the fit from (3.5) is remarkably accurate.

3.2. *Mean profiles and the maximum principle*

In turbulent RBC flows, one expects the temperature to be well mixed in the interior, so that the profile consists, to a good approximation, of steep boundary layers near the top and bottom plates, and a region of constant temperature in the middle. We anticipate the same behaviour will hold for the azimuthal velocity v relative to the x_3 direction. Moreover, since (2.1c) is an explicit advection–diffusion equation, the temperature satisfies a maximum principle, i.e. T is bounded by its values at the walls,

$$T_0 \leq T \leq T_0 + \delta T, \tag{3.7}$$

https://doi.org/10.1017/jfm.2020.718 Published online by Cambridge University Press

at any point in the volume. This arises because near a maximum the first derivative vanishes and the second is negative, so diffusion will act to reduce it. For RBC, this indicates that heat cannot pile up at the walls beyond that supplied by the boundary condition. Translated to RPC, the corresponding statement will address the relation between the downstream velocity and its value at the walls. A velocity field that lies outside the values provided by the boundary conditions is referred to in the literature as a backflow event. Existence of such backflow events has been a matter of controversy which was settled with the explicit demonstration of such events by Lenaers *et al.* (2012).

To see how the maximum principle applies to RPC, we let $v = -2\Omega x_3 + \tilde{v}$, so that $\tilde{v}$ satisfies the advection–diffusion equation $\partial_t \tilde{v} + (\boldsymbol{u} \cdot \boldsymbol{\nabla})\tilde{v} = \nu \Delta \tilde{v}$. This perturbative velocity field $\tilde{v}$ satisfies a maximum principle, i.e. its extreme values occur only at $x_3 = 0$ or $x_3 = d$. This can be stated succinctly as $2\Omega d \leq \tilde{v} \leq U$, or $0 \leq v \leq U$ for the original azimuthal velocity component (assuming a positive U). This implies that in this setting there is no backflow, i.e. the azimuthal velocity has a constant sign, and events like the ones observed by Lenaers *et al.* (2012) cannot occur in 2D3C RPC. It would be of significant interest to determine if such events can occur for 3-D RPC or even for the full TCF system. If so, one must question whether these events are present only for full 3-D flows or if the current restriction in RPC is unique.

3.3. *Free-slip boundary conditions*

Although the no-slip boundary condition is clearly the physically motivated choice for TCF, and, hence, for RPC as well, there is still some interest in considering the free-slip condition, although there is less immediate physical motivation for this. Indeed, Rayleigh (1916) invoked free-slip conditions for mathematical convenience:

> *... for a further condition we should probably prefer* $\mathrm{d}w/\mathrm{d}z = 0$ [no-slip]*, corresponding to a fixed solid wall. But this entails much complication, and we may content ourselves with the supposition* $\mathrm{d}^2w/\mathrm{d}z^2 = 0$ [free-slip]*...*

Thus, in the interest of reducing such 'complication' due to the no-slip condition, we will consider stress-free (free-slip) boundary conditions on the plates for u and w. As mentioned previously, this is presented in the form $w = 0$ and $\partial_3 u = 0$ at $x_3 = 0$ and 1. Incompressibility then implies that the vorticity in the x_2 direction defined by $\omega_2 = \partial_1 w - \partial_3 u$ vanishes at these boundaries as well. This leads to an enstrophy balance, where the enstrophy is defined as the square of the L^2 norm of ω_2, i.e. $\|\omega_2\|_2^2$. This restriction which we consider in this section only, does not reflect on any other aspect of the system as described above.

As shown by Whitehead & Doering (2011), this enstrophy balance, coupled with a uniform bound on $w(x_3)$ near the boundary and a piece-wise linear, monotonic temperature profile, will yield a bound on the Nusselt number in RBC of the form $Nu_T \leq cRa^{5/12}$. Translated into the RPC system, this becomes

$$Nu_S \lesssim R_\Omega + Re_S^{5/6}(1 - R_\Omega)^{17/12} R_\Omega^{5/12}, \tag{3.8}$$

which will have a maximum as $Re_S \to \infty$ for $R_{\Omega,m} = 5/22 \sim 0.227$ by (3.6). This is the only setting to date for which the scaling of Nu_S is sublinear with respect to Re_S, deviating from the anticipated Re_S^1 scaling, and, hence, there is no anomalous dissipation in this setting. Remarkably this scaling affects the Re_S-dependence, but it has little influence on the location of the maxima in R_Ω.

https://doi.org/10.1017/jfm.2020.718 Published online by Cambridge University Press

4. Conclusions and discussion

We have analysed some consequences of an exact relationship between 2-D RBC and 2D3C RPC, the limit of 2-D TCF flow for large radii relative to the gap width. These two problems can be mapped onto each other via an identification of corresponding fields and a change of variables as defined in table 1. This converts the well-known analogy between these systems to an exact comparison. Comparison of these conclusions to previous numerical and experimental observations indicate that some of the results apply to the full 3-D situation. For instance, the additional factor in the relation between heat and momentum transport gives an asymmetry in the location of the maximum as a function of R_Ω, which agrees well with observations on fully 3-D flows.

Restricting to the 2-D setting removes the possibility of a backflow event due to a maximum principle, and, for the specific choice of free-slip boundary conditions, there is a sublinear scaling of torque with shear Reynolds number. In both cases, it should be interesting to explore further how higher dimensions and modifications of boundary conditions can cause deviations from these 2-D relations. More generally, the differences in the equations of motion between the 2-D and 3-D cases may point to other observables in which fully 3-D RBC and RPC differ.

Acknowledgements

Prior to completion of this paper, the first author, our dear friend B. Eckhardt, died rather suddenly. Bruno inspired the research reported here and contributed the central ideas to the study. This is not the place to describe Bruno's lasting contributions to the study of nonlinear dynamics and turbulence; suffice it to say that his loss has been and will be deeply felt not only by his closest collaborators, but by all who have an interest in the field. Our effort to complete this paper is dedicated to his memory. We also thank H. Brauckmann for providing the data necessary to produce figure 2. This work was supported in part by the US National Science Foundation via awards DMS-1515161 and DMS-1813003, and the Simons Foundation through award number 586788. This work was initiated at the Institute for Pure & Applied Mathematics, Mathematics of Turbulence programme during the fall of 2014, and we appreciate the persisting influence of that programme.

Declaration of interests

The authors report no conflict of interest.

References

Ahlers, G. & Behringer, R. P. 1978 Evolution of turbulence from Rayleigh–Bénard instability. *Phys. Rev. Lett.* **40** (11), 712–716.

Bradshaw, P. 1969 The analogy between streamline curvature and buoyancy in turbulent shear flow. *J. Fluid Mech.* **36**, 177–191.

Brauckmann, H. J., Eckhardt, B. & Schumacher, J. 2017 Heat transport in Rayleigh–Bénard convection and angular momentum transport in Taylor–Couette flow: a comparative study. *Phil. Trans.* A **375** (2089), 20160079.

https://doi.org/10.1017/jfm.2020.718 Published online by Cambridge University Press

BRAUCKMANN, H. J., SALEWSKI, M. & ECKHARDT, B. 2016 Momentum transport in Taylor–Couette flow with vanishing curvature. *J. Fluid Mech.* **790**, 419–452.

BUSSE, F. H. 1969 Bounds on transport of mass and momentum by turbulent flow between parallel plates. *Z. Angew. Math. Phys.* **20** (1), 1–14.

CHANDRASEKHAR, S. 1961 *Hydrodynamics and Hydro-Magnetic Stability*. Clarendon Press.

CHOSSAT, P. & IOOSS, G. 2012 *The Couette–Taylor Problem*. Springer.

CONSTANTIN, P. 1994 Geometric statistics in turbulence. *SIAM Rev.* **36** (1), 73–98.

DOERING, C. R. & CONSTANTIN, P. 1992 Energy dissipation in shear driven turbulence. *Phys. Rev. Lett.* **69** (11), 1648–1651.

DOERING, C. R. & CONSTANTIN, P. 1994 Variational bounds on energy dissipation in incompressible flows: shear flow. *Phys. Rev.* E **49**, 4087–4099.

DOERING, C. R. & CONSTANTIN, P. 1996 Variational bounds on energy dissipation in incompressible flows. III. Convection. *Phys. Rev.* E **53** (6), 5957–5981.

DOERING, C. R., OTTO, F. & REZNIKOFF, M. G. 2006 Bounds on vertical heat transport for infinite-Prandtl-number Rayleigh–Bénard convection. *J. Fluid Mech.* **560**, 229–241.

DUBRULLE, B., DAUCHOT, O., DAVIAUD, F., LONGARETTI, P.-Y., RICHARD, D. & ZAHN, J.-P. 2005 Stability and turbulent transport in Taylor–Couette flow from analysis of experimental data. *Phys. Fluids* **17** (9), 095103.

DUBRULLE, B. & HERSANT, F. 2002 Momentum transport and torque scaling in Taylor–Couette flow from an analogy with turbulent convection. *Eur. Phys. J.* B **26**, 379–386.

ECKHARDT, B., GROSSMANN, S. & LOHSE, D. 2007*a* Fluxes and energy dissipation in thermal convection and shear flows. *Europhys. Lett.* **78** (2), 7.

ECKHARDT, B., GROSSMANN, S. & LOHSE, D. 2007*b* Torque scaling in turbulent Taylor–Couette flow between independently rotating cylinders. *J. Fluid Mech.* **581**, 221–250.

EZETA, R., SACCO, F., BAKHUIS, D., HUISMAN, S. G., OSTILLA-MÓNICO, R., VERZICCO, R., SUN, C. & LOHSE, D. 2020 Double maxima of angular momentum transport in $\eta = 0.91$ TC turbulence. arXiv:2006.03528.

FAISST, H. & ECKHARDT, B. 2000 Transition from the Couette–Taylor system to the plane Couette system. *Phys. Rev.* E **61** (6 Pt B), 7227–7230.

GOLLUB, J. P. & SWINNEY, H. L. 1975 Onset of turbulence in a rotating fluid. *Phys. Rev. Lett.* **35** (14), 927–930.

HOWARD, L. N. 1963 Heat transport by turbulent convection. *J. Fluid Mech.* **17** (3), 405–432.

HOWARD, L. N. 1972 Bounds on flow quantities. *Annu. Rev. Fluid Mech.* **4**, 473–494.

JEFFREYS, H. 1928 Some cases of instability in fluid motion. *Proc. R. Soc. Lond.* A **118**, 195–208.

LENAERS, P., LI, Q., BRETHOUWER, G., SCHLATTER, P. & ÖRLÜ, R. 2012 Rare backflow and extreme wall-normal velocity fluctuations in near-wall turbulence. *Phys. Fluids* A **24** (3), 035110.

MANNEVILLE, P. 2010 *Instabilities, Chaos and Turbulence*. Imperial College Press.

NAGATA, M. 1986 Bifurcations in Couette flow between almost corotating cylinders. *J. Fluid Mech.* **169**, 229–250.

NAGATA, M. 2013 A note on the mirror-symmetric coherent structure in plane Couette flow. *J. Fluid Mech.* **727**, R1.

NICKERSON, E. C. 1969 Upper bounds on torque in cylindrical Couette flow. *J. Fluid Mech.* **38** (4), 807–815.

OTTO, F. & SEIS, C. 2011 Rayleigh–Bénard convection: improved bounds on the Nusselt number. *J. Math. Phys.* **52**, 083702.

PLASTING, S. C. & KERSWELL, R. R. 2003 Improved upper bound on the energy dissipation rate in Plane Couette flow: the full solutions to Busse's problem and the Constantin–Doering–Hopf problem with one-dimensional background fields. *J. Fluid Mech.* **477**, 363–379.

RAYLEIGH, LORD 1916 On convection currents in a horizontal layer of fluid, when the higher temperature is on the under side. *Phil. Mag. J. Sci.* **32** (192), 529–546.

SALEWSKI, M. & ECKHARDT, B. 2015 Turbulent states in plane Couette flow with rotation. *Phys. Fluids* A **27** (4), 045109.

SPIEGEL, E. A. 1963 A generalization of the mixing-length theory of thermal convection. *Astrophys. J.* **138**, 216–225.

https://doi.org/10.1017/jfm.2020.718 Published online by Cambridge University Press

VERONIS, G. 1970 The analogy between rotating and stratified fluids. *Annu. Rev. Fluid Mech.* **2**, 37–66.

WHITEHEAD, J. P. & DOERING, C. R. 2011 The ultimate regime of two-dimensional Rayleigh–Bénard convection with stress-free boundaries. *Phys. Rev. Lett.* **106**, 244501.

WHITEHEAD, J. P. & DOERING, C. R. 2012 Rigid rigorous bounds on heat transport in a slippery container. *J. Fluid Mech.* **707**, 241–259.

https://doi.org/10.1017/jfm.2020.718 Published online by Cambridge University Press